Dissociable neural information dynamics of perceptual integration and differentiation during bistable perception

Andrés Canales-Johnson[1,2,3*], Alexander J. Billig[2,4], Francisco Olivares[3], Andrés Gonzalez[3], María del Carmen Garcia[5], Walter Silva[5], Esteban Vaucheret[5], Carlos Ciraolo[5], Ezequiel Mikulan[6], Agustín Ibanez[6,7,8,9,10,11], Valdas Noreika[1,2], Srivas Chennu[12,13] and Tristan A. Bekinschtein[1,2]

1 Department of Psychology, University of Cambridge, Cambridge, United Kingdom.

2 Medical Research Council Cognition and Brain Sciences Unit, Cambridge, United Kingdom.

3 Faculty of Psychology, Universidad Diego Portales, Santiago, Chile.

4 Brain and Mind Institute, University of Western Ontario, London, Canada.

5 Programa de Cirugía de Epilepsia, Hospital Italiano de Buenos Aires, Argentina.

6 Laboratory of Experimental Psychology and Neuroscience (LPEN), Institute of Cognitive and Translational Neuroscience (INCyT), INECO Foundation, Favaloro University, Buenos Aires, Argentina.

8 National Scientific and Technical Research Council (CONICET), Buenos Aires, Argentina.

9 Universidad Autónoma del Caribe, Barranquilla, Colombia

10 Center for Social and Cognitive Neuroscience (CSCN), School of Psychology, Universidad Adolfo Ibáñez, Santiago, Chile.

11 Centre of Excellence in Cognition and its Disorders, Australian Research Council (ACR), Sydney, Australia.

12 School of Computing, University of Kent, Chatham Maritime, United Kingdom.

13 Department of Clinical Neurosciences, University of Cambridge, United Kingdom.

* Correspondence:

Andres Canales-Johnson, PhD

Department of Psychology

University of Cambridge

Downing Site, CB2 3EB

Cambridge, United Kingdom.

afc37@cam.ac.uk

Funding

This research was supported by a Wellcome Trust Biomedical Research Fellowship WT093811MA (TAB), the Chilean National Fund for Scientific and Technological Development Grant 1130920 (ACJ), the Argentinean National Research Council for Science and Technology, and the Argentinean Agency for National Scientific Promotion, FONCyT -PICT 2012-0412 and FONCyT-PICT 2012-1309.

Author's contributions

Conceived and designed the experiments: ACJ, TAB. Performed the experiments: ACJ, FO, AG, EM. Analysed the data: ACJ. Contributed reagents/materials/analysis tools: AB, SC. Gave access to clinical patient: MCG, WS, EV, CC. Wrote the paper: ACJ, AB, AI, VN, SC, TAB.

Acknowledgments

We thank Robert Carlyon, Simon van Gaal, Anat Arzi, William J. Harrison, Daniel Bor, David Huepe and Michael Schartner for contributing to valuable discussion and insights. This manuscript is dedicated to the memory of Prof. Walter J. Freeman (1927 - 2016) whose pioneering work on Neurodynamics has inspired and ignited countless meaningful insights during the execution of this project.

Conflict of Interest

None declared.

ABSTRACT

At any given moment, we experience a perceptual scene as a single whole and yet we may distinguish a variety of objects within it. This phenomenon instantiates two properties of conscious perception: integration and differentiation. Integration to experience a collection of objects as a unitary percept, and differentiation to experience these objects as distinct from each other. Here we evaluated the neural information dynamics underlying integration and differentiation of perceptual contents during bistable perception. 30 participants listened to a sequence of tones (auditory bistable stimuli) experienced either as a single stream (perceptual integration) or as two parallel streams (perceptual differentiation) of sounds. We computed neurophysiological indices of information-integration and information-differentiation with electroencephalographic and direct brain recordings. In both, the integrated percept was associated with an increase in information-integration and a decrease in differentiation across frontoparietal regions, whereas the opposite pattern was observed for the differentiated percept. There were no changes for externally driven content of perception control task). Furthermore, traditional measures of neural oscillatory integration (phase synchronization) and frequency signalled percept stability but not percept type. We demonstrated that perceptual integration and differentiation can be mapped to theoretically-motivated neural information signatures, suggesting a one-to-one relationship between phenomenology and neurophysiology.

Keywords: phenomenal consciousness, bistable perception, information integration, information differentiation, EEG, auditory streaming

INTRODUCTION

Phenomenologically, conscious experience does not only depend on the external information we receive from the environment, but also on internal information that is independent of sensory stimulation. This dissociation between external stimulation and conscious experience is observed in several visual and auditory perceptual illusions in which two or more internally driven percepts alternate under unchanging external stimulation (Sterzer et al., 2009). Moreover, conscious experience cannot be divided into discrete independent components (i.e., it is perceptually integrated), but it can contain an assortment of events and objects (i.e., it is perceptually differentiated) (Tononi et al., 2016). Thus, while integration is the property of experiencing a collection of objects as a unitary percept, differentiation is the property of experiencing these objects as distinct from each other. What are the neural markers of the integration and differentiation of internally driven perceptual contents? We propose that integration and differentiation of internally driven percepts can be neurophysiologically investigated during auditory bistability. During the particulary form of auditory bistability employed here, an invariant sequence of tones is experienced as forming either an integrated percept (one stream) or a differentiated percept (two streams) (Snyder et al., 2012) (Figure 1).

Neurophysiologically, conscious experience is thought to require the joint presence of information integration and information differentiation (Oizumi et al., 2014; Tononi et al., 2016). In particular, the emergence of conscious percepts is believed to involve the integration of information coming from frontal and parietal brain areas to form a phenomenologically unified whole (Dehaene and Changeux, 2011; Dehaene et al., 2014; Tononi et al., 2016). Therefore, a reasonable assumption is that the integrated percept (one stream, in the case of this experiment) should be associated with correspondingly higher neural information integration (NII). Recently, NII has been empirically measured in a direct manner by computing the amount of information shared between long-distance EEG signals, and it has been used to discriminate between vegetative and minimally conscious patients (King et al., 2013; Sitt et al., 2014). This NII measure can detect non-oscillatory coupling between signals as compared to classical measures of neural oscillatory integration (NOI) such as phase synchronization. In the case of auditory bistability, we expect higher neural information integration for the perceptually integrated (one-stream) percept compared to the perceptually differentiated (two-streams) percept, as the former would require information about tones of two different frequencies to form a single, integrated percept.

Complementary to NII, empirical indices of neural information differentiation (NID) have been used to separate levels of consciousness by estimating the degree of compressibility of EEG signals (Casali

et al., 2013; Sitt et al., 2014; Schartner et al., 2015, 2017). For instance, a decrease in NID has been observed in patients in vegetative states compared to minimally conscious states (Sitt et al., 2014), showing that differentiation of neural information is associated with a cognitively more advanced state of consciousness, as clinically defined. On the other hand, the only study providing a preliminary indication that neurophysiological differentiation might be related to perceptual processes is an fMRI study (Boly et al., 2015), showing that NID was highest when participants watched a coherent movie, intermediate when scenes were scrambled, and minimal for 'TV noise'. However, it is unclear whether neurophysiological differentiation was specifically related to conscious awareness since factors such as low-level visual processing, expectations and top-down attention might have influenced the differences observed between conditions. During auditory bistability, we can specifically evaluate perceptual differentiation directly since what is changing is not the stimulus itself but how it is subjectively experienced. If the neural information associated with a conscious percept is highly differentiated, NID is expected to be high since information should be less compressible. In contrast, neural differentiation is expected to be low if EEG signals are processing information in a stereotypical way because information is highly redundant (easily compressed). Following this rationale, we expect that the differentiated (two-stream) percept should be associated with higher neural information differentiation.

In addition, there is ample and rapidly growing evidence that endogenous or 'ongoing' brain activity in the gamma band (30-70 Hz) is neither meaningless nor random but instead carries functional information largely determining the way incoming stimuli are interpreted (Engel et al., 2001, 2013; Varela et al., 2001; Freeman, 2015). For instance, studies of the visual system have shown that neural oscillatory integration (NOI) in the gamma-band is involved in the alternation between visual conscious percepts (Doesburg et al., 2005; Hipp et al., 2012). Thus, drawing upon these results and a wealth of previous research that has identified gamma band activity as relevant for conscious perception (Melloni et al., 2007; Engel et al., 2013; Levy et al., 2015), we analyse here information and oscillatory dynamics of ongoing activity in the gamma band. However, we specifically evaluate the theoretical prediction (Koch et al., 2016) that information dynamics (NII and NID) but not oscillatory dynamics (NOI) of ongoing activity underpin phenomenological integration and differentiation.

By measuring high-density scalp EEG and Local Field Potentials (LFP) from direct cortical recordings in humans, we tested the hypothesis that during the formation of internally driven percepts, conscious experience goes along with neurophysiological indices of information processing. Specifically, we predict that the perceptually integrated content corresponds to high frontoparietal neural information integration in the gamma band and conversely, the perceptually differentiated content is associated with high neural information differentiation within frontal and parietal regions.

Materials and Methods

Healthy participants and patient

Twenty-nine right-handed healthy participants (14 males; mean ± SD age = 21.30 ± 2.2 years) and one left-handed epileptic patient (female; 29 years) gave written informed consent to take part in the experiment. The study was approved by the institutional ethics committee of the Faculty of Psychology of Universidad Diego Portales (Chile) and the Institutional Ethics Committee of the Hospital Italiano de Buenos Aires, Argentina, in accordance with the Declaration of Helsinki. The patient suffered from drug-resistant epilepsy from the age of 8 years and was offered surgical intervention to alleviate her intractable condition. Drug treatment at the time of implantation included 600 mg/d oxcarbazepine, 200 mg/d topiramate, and 750 mg/d levetiracetam. Computed tomography (CT) and magnetic resonance imaging (MRI) scans were acquired after insertion of depth electrodes. The patient took part in the current study one day before the surgery. She was attentive and cooperative during testing, and her cognitive performance before and one week after the implantation was indistinguishable from healthy volunteers. The patient was specifically recruited for this study because she was implanted with electrodes covering frontal and parietal regions.

Stimuli

In the endogenous condition, a high-frequency pure tone A alternated with a low-frequency pure tone B, in a repeating ABA- pattern. The frequency of A was 587 Hz and that of B was 440 Hz (5 semitones difference). The duration of each tone was 120 ms. The silence ('-') that completed the ABA… pattern was also 120 ms long, thus making the A tones isosynchronous (Pressnitzer and Hupé, 2006). In the exogenous (control) condition, the ABA- pattern alternated with an AB-- pattern. This second pattern had the same parameters (frequencies and duration) and same silence duration as the ones used for the endogenous condition (ABA- pattern). Duration of both patterns (ABA- and AB--) were randomly set between 4-8 seconds, which suppressed the effect of endogenous bistability, and ABA- was most often perceived as one stream, whereas AB—was largely perceived as two streams.

For both experimental conditions, the auditory stimuli consisted of 4 min long sequences. Each sequence was presented 12 times per condition with a 30 second pause between sequences. Stimuli were presented binaurally using Etymotics ER-3A earphones, and the sound level was individually adjusted to a comfortable level. The order of experimental conditions was counterbalanced between participants.

Experimental conditions

There were two experimental conditions. In the endogenous condition (bistability), we used a bistable auditory (Carlyon et al., 2001; Gutschalk et al., 2005; Pressnitzer and Hupé, 2006)Participants listened to a pattern of three tones (ABA) separated by a silence ('-') (see Stimuli section) that are experienced either as a one-stream percept or as a two-streams percept (Figure 1a). Participants were instructed to press a button with one hand when perceiving that the one-stream percept had fully changed into two streams and a second button with the other hand when perceiving that the two-streams percept had fully changed into one stream (Figure 1, middle panel). In the exogenous condition (control), participants listened to two alternating patterns of three (ABA) and two (AB) tones separated by a period of silence ('-') (see Stimuli section). As in the endogenous conditions, participants were instructed to press a button with one hand when perceiving that ABA- had fully changed into AB- and another button with the other hand when pattern AB- had fully changed into ABA-. The exogenous condition allowed us to characterize the dynamics of neural activity specifically related to external changes in the stimuli (the two alternating patterns) and to contrast them with the dynamics of internal neural activity elicited by the endogenous condition (bistability). The endogenous and exogenous conditions used physically similar stimuli, as described in the Stimuli section, with the latter sometimes having one fewer A tone. Because the analysis windows were not time-locked to the stimuli, differences in the evoked responses to specific tones are unlikely to account for the observed pattern of results.

Electroencephalography (EEG) recordings, pre-processing and analysis

EEG signals were recorded with 128-channel HydroCel Sensors using a GES300 Electrical Geodesic amplifier at a sampling rate of 500 Hz using the NetStation software. During recording and analyses, the electrodes' average was used as the reference electrode. Two bipolar derivations were designed to monitor vertical and horizontal ocular movements. Following Chennu *et al* (Chennu et al., 2014), data from 92 channels over the scalp surface were retained for further analysis. Channels on the neck, cheeks and forehead, which reflected more movement-related noise than signal, were excluded. Eye movement contamination and other artefacts were removed from data before further processing using an independent component analysis(Delorme and Makeig, 2004). All conditions yielded at least 91% of artefact-free trials. Trials that contained voltage fluctuations exceeding ± 200 µV, transients exceeding ± 100 µV, or electro-oculogram activity exceeding ± 70 µV were rejected. The EEGLAB MATLAB toolbox was used for data pre-processing and pruning(Delorme and Makeig, 2004). MATLAB open source software FieldTrip (Oostenveld et al., 2011) and customized scripts were used for calculating NII, NID and NOI measures.

Local field potential (LFP) recordings and pre-processing

Direct cortical recordings were obtained from semi-rigid, multi-lead electrodes that were implanted in the patient. The electrodes had a diameter of 0.8 mm and consisted of 5, 10 or 15 contact leads that were 2-mm wide and 1.5-mm apart (DIXI Medical Instruments). The electrode strips were implanted in different regions of the frontal, temporal, central and parietal cortices and subcortical structures. For the purposes of the current study, local field potentials (LFP) were analysed from the left middle frontal gyrus and left superior parietal lobe. MNI coordinates of the depth electrodes were obtained from MRI and CT images using SPM (Friston, 2006) and MRIcron (Rorden and Brett, 2000) software. The recordings were sampled at 1024 Hz and down-sampled to 500 Hz for further analysis. The exact MNI coordinates and cortical regions of the selected electrodes are reported in Table 1. Open-source BrainNet Viewer software was used for visualization of selected electrodes (Xia et al., 2013).

Analysis of ongoing neural activity

A classical experimental approach for studying endogenous, or “ongoing” activity in the EEG related to internal fluctuations during cognitive tasks is by analysing the EEG window before the onset of motor responses when participants report internal changes. This approach has been used for studying neural signatures of conscious awareness, such as in bistable perception (Parkkonen et al., 2008), binocular rivalry (Doesburg et al., 2005; Frässle et al., 2014) and intrusions of consciousness (Noreika et al., 2015). Here, ongoing EEG and LFP activity (not time-locked to stimuli) preceding the onset of each response (button press), and presumed to span the change in perception, was analysed in terms of connectivity (NII and NOI) and complexity (NII).

Window size selection was based on the following procedure. In the exogenous condition, we calculated the mean reaction times in the group of healthy participants (M = 1342 ms; SD = 101 ms). Then, in the endogenous condition, we calculated the minimum temporal gap between responses such that epochs would not overlap (2500 ms). Since mean reaction times in the exogenous condition corresponded to roughly half of the minimal window size of the endogenous condition, we selected a 2500 ms window for both conditions (from -2500 to 0 ms relative to button press) (Figure 1, lower panel). Importantly, this window included the onset of the exogenous auditory patterns ('ABA-' and 'AB--'), making the exogenous and endogenous conditions comparable from a stimulus perspective. The same procedure was repeated for the intracranial data (reaction times in the exogenous condition: M = 1380 ms, SD = 79 ms; window size in the endogenous conditions: 2500 ms).

For statistical analyses (see below), two time windows of 500 ms were selected based on the exogenous condition. A window after the change between auditory percepts (after-change window (AC)) was defined based on the mean reaction times at the group level (from -1342 to -842 ms). A

second time window was defined at the epoch onset (before-change window (BC); from -2500 to -2000 ms). The rationale behind the latencies of both time windows was to select the periods when both externally driven percepts remained stable. The same window lengths and latencies were used for the endogenous condition (Figure 1).

Phase synchronization

We quantified phase coherence between pairs of electrodes as a measure of dynamical linear coupling among signals oscillating in the same frequency band. Phase synchronization analysis proceeds into two steps: (i) estimation of the instantaneous phases and (ii) quantification of the phase locking.

Estimation of the instantaneous phases

To obtain the instantaneous phases φ of the neural signals, we used the Hilbert transform approach (Foster et al., 2016). The analytic signal $\xi(t)$ of the univariate measure $x(t)$ is a complex function of continuous time t defined as:

$$(1) \qquad \xi(t) = x(t) + ix_h(t) = a_\xi(t)e^{i\varphi_\xi(t)}$$

where the function $x_h(t)$ is the Hilbert transform of $x(t)$:

$$(2) \qquad x_h(t) = \frac{1}{\pi} P.V. \int_{-\infty}^{+\infty} \frac{x(t)}{t-\tau} d\tau$$

P.V. indicates that the integral is taken in the sense of Cauchy principal value. Sequences of digitized values give a trajectory of the tip of a vector rotating counterclockwise in the complex plane with elapsed time.

The vector norm at each digitizing step t is the state variable for instantaneous amplitude $a_\xi(t)$. This amplitude corresponds to the length of the vector specified by the real and imaginary part of the complex vector computed by Pythagoras' law and is equivalent to the magnitude of the observed oscillation at a given time and frequency point.

$$(3) \qquad a_\xi(t) = \sqrt{x(t)^2 + ix_h(t)^2}$$

and the arctangent of the angle of the vector with respect to the real axis is the state variable for instantaneous phase $\varphi_x(t)$.

$$(4) \qquad \varphi_x(t) = arctg \frac{ix_h(t)}{x(t)}$$

The instantaneous phase $\varphi_x(t)$ of $x(t)$ is taken equal to $\varphi_\xi(t)$. Identically, the phase $\varphi_y(t)$ is estimated from $y(t)$. This phase is thus the angle of the vector specified by the real and imaginary components. For a given time and frequency point, it corresponds to a position inside the oscillation cycle (peak, valley, rising, or falling slope).

The instantaneous phase, although defined uniquely for any kind of signal to which the Hilbert transform can be applied, is difficult to interpret physiologically for broadband signals. For this reason, a standard procedure is to consider only narrow-band phase synchronization by estimating an instantaneous phase for successive frequency bands, which are defined by band-pass filtering the time series(Le Van Quyen et al., 2001). Thus, for each trial and electrode, the instantaneous phase of the signal was extracted at each frequency of the interval 1- 60 Hz (in 1-Hz steps) by computing the Hilbert transform using a zero phase shift non-causal finite impulse filter.

Neural oscillatory integration: weighted phase lag index (wPLI)

Phase synchronization is often calculated from the phase or the imaginary component of the complex cross-spectrum between the signals measured at a pair of channels. For example, the well-known Phase Locking Value (PLV) (Lachaux et al., 1999) is obtained by averaging the exponential magnitude of the imaginary component of the cross-spectrum. However, such phase coherence indices derived from EEG data are affected by the problem of volume conduction, and as such they can have a single dipolar source, rather than a pair of distinct interacting sources, producing spurious coherence between spatially disparate EEG channels. The Phase Lag Index (PLI), first proposed by Stam *et al* (Stam et al., 2007) attempts to minimize the impact of volume conduction and common sources inherent in EEG data, by averaging the signs of phase differences, thereby ignoring average phase differences of 0 or 180 degrees. This is based on the rationale that such phase differences are likely to be generated by volume conduction of single dipolar sources. However, despite being insensitive to volume conduction, PLI has a strong discontinuity in the measure, which causes it to be maximally sensitive to noise.

The Weighted Phase Lag Index (wPLI) (Vinck et al., 2011) addresses this problem by weighting the signs of the imaginary components by their absolute magnitudes. Further, as the calculation of wPLI also normalises the weighted sum of signs of the imaginary components by the average of their absolute magnitudes, it represents a dimensionless measure of connectivity that is not directly influenced by differences in spectral or cross-spectral power. For these reasons, we employed the wPLI measure to estimate connectivity in our data. The wPLI index ranges from 0 to 1, with value 1 indicating perfect synchronization (phase difference is perfectly constant throughout the trials) and

value 0 representing total absence of synchrony (phase differences are random). For each trial and pair of electrodes, wPLI was estimated using a 500 ms sliding window with 2 ms time step, i.e. with a 96% overlap between two adjacent windows.

Neural information integration: weighted symbolic mutual information (wSMI)

In order to quantify the coupling of information flow between electrodes we computed the weighted symbolic mutual information (wSMI) (King et al., 2013; Sitt et al., 2014). It assesses the extent to which the two signals present joint non-random fluctuations, suggesting that they share information. wSMI has three main advantages: (i) it allows for a rapid and robust estimation of the signals' entropies; (ii) it provides an efficient way to detect non-linear coupling; and (iii) it discards the spurious correlations between signals arising from common sources, favouring non-trivial pairs of symbols. For each trial, wSMI is calculated between each pair of electrodes after the transformation of the EEG and LFPs signals into sequence of discrete symbols discrete symbols defined by the ordering of k time samples separated by a temporal separation τ (King et al., 2013). The symbolic transformation depends on a fixed symbol size (k = 3, that is, 3 samples represent a symbol) and a variable τ between samples (temporal distance between samples) which determines the frequency range in which wSMI is estimated(Sitt et al., 2014). In our case, we chose τ = 32 and 6 ms to isolate wSMI in alpha ($wSMI_{\alpha}$) and gamma ($wSMI_{\gamma}$) bands respectively. The frequency specificity *f* of wSMI is related to k and τ as:

$$f = 1000 / (\tau * k)$$

As per the above formula, with a kernel size k of 3, τ values of 32 and 6 ms hence produced a sensitivity to frequencies near 55 Hz (gamma) and 10 Hz (alpha) range, respectively.

wSMI was estimated for each pair of transformed EEG and LFPs signals by calculating the joint probability of each pair of symbols. The joint probability matrix was multiplied by binary weights to reduce spurious correlations between signals. The weights were set to zero for pairs of identical symbols, which could be elicited by a unique common source, and for opposite symbols, which could reflect the two sides of a single electric dipole. wSMI is calculated using the following formula:

$$wSMI(X,Y) = \frac{1}{\log(k!)} \sum_{x \in X} \sum_{y \in Y} w(x,y)\, p(x,y) \log\left(\frac{p(x,y)}{p(x)p(y)}\right)$$

where *x* and *y* are all symbols present in signals *X* and *Y* respectively, w*(x,y)* is the weight matrix and *p(x,y)* is the joint probability of co-occurrence of symbol *x* in signal *X* and symbol *y* in signal *Y*. Finally, *p(x)* and *p(y)* are the probabilities of those symbols in each signal and *K*! is the number of symbols - used to normalize the mutual information (MI) by the signal's maximal entropy. Temporal evolution of wSMI was calculated using a 500 ms sliding window with 2 ms time step, i.e. with a 96% overlap between two adjacent windows.

Neural information differentiation: Kolmogorov-Chaitin complexity (K complexity)

Kolmogorov-Chaitin complexity quantifies the algorithmic complexity (Kolmogorov, 1965; Chaitin, 1974) of an EEG signal by measuring its degree of redundancy (Sitt et al., 2014; Schartner et al., 2015, 2017). Algorithmic complexity of a given EEG sequence can be described as the length of shortest computer program that can generate it. A short program corresponds to a less complex sequence. K complexity was estimated by quantifying the compression size of the EEG using the Lempel-Ziv zip algorithm (Lempel and Ziev, 1976).

Algorithmic information theory has been introduced by Andreï Kolmogorov and Gregory Chaitin as an area of interaction between computer science and information theory. The concept of algorithmic complexity or Kolmogorov-Chaitin complexity (K complexity) is defined as the shortest description of a string (or in our case a time series *X*). That is to say, K complexity is the size of the smallest algorithm (or computer program) that can produce that particular time series. However, it can be demonstrated by *reductio ad absurdum* that there is no possible algorithm that can measure K complexity (Chaitin, 1995). To sidestep this issue, we can estimate an upper-bound value of K complexity(*X*). This can be concretely accomplished by applying a lossless compression of the time series and quantifying the compression size. Capitalizing on the vast signal compression literature, we heuristically used a classical open-source compressor gzip (Salomon, 2004) to estimate K complexity(*X*). It is important to standardize the method of representation of the signal before compression in order to avoid non-relevant differences in complexity. Specifically, to compute K complexity(*X*):

1. The time series were transformed into sequences of symbols. Each symbol represents, with identical complexity, the amplitude of the corresponding channel for each time point. The number of symbols was set to 32 and each one corresponds to dividing the amplitude range of that given channel into 32 equivalent bins. Similar results have been obtained with binning ranging from 8 to 128 bins (Sitt et al., 2014).
2. The time series were compressed using the compressLib library for Matlab, this library implements the gzip algorithm to compress Matlab variables.

3. K complexity(X) was calculated as the size of the compressed variable with time series divided by the size of the original variable before compression. Our premise is that, the bigger the size of the compressed string, the more complex the structure of the time series, thus potentially indexing the complexity of the electrical activity recorded at a sensor.

For each trial and channel, K complexity was estimated using a 500 ms sliding window with 2 ms time step, i.e. with a 96% overlap between two adjacent windows.

EEG electrode cluster analysis and epoch correction

Clusters of electrodes were selected for complexity analysis and connectivity analysis (wPLI and wSMI) by selecting the canonical frontal, parietal, right-temporal and left-temporal electrodes. In the case of spectral power analysis, power values within frontal and parietal electrodes were averaged per condition and participant. In the case of frontoparietal wPLI, wSMI and K complexity analyses, we calculated the mean connectivity that every electrode of the frontal cluster shared with every electrode of the parietal cluster. Connectivity values between pairs of electrodes and between parietal pairs of parietal electrodes were discarded from the analysis. Similarly, in the case of temporotemporal connectivity analyses, we calculated the mean connectivity that every electrode of the of the right-temporal cluster shared with every electrode of the left-temporal cluster, discarding connectivity values within pairs of right-temporal electrodes and pairs of left-temporal electrodes. This procedure allows us to specifically test the role of long-distance interactions (frontoparietal and temporotemporal) during bistable perception. K complexity, wSMI and wPLI values of the corresponding regions of interest were averaged per condition and participant.

In order to make both conditions comparable (endogenous vs exogenous), after transforming data into complexity (K complexity) and connectivity (wPLI and wSMI) time series and creating the corresponding electrode clusters, we subtracted the mean activity between -2500 to -700 ms from each data point per epoch and condition. Motor-related activity in the gamma band has been reported ~-200 ms before the button press during bistable perception (Basirat et al., 2008). Thus, although it is a common procedure to analyse response-evoked activity by correcting epochs using the mean of the entire window (Doesburg et al., 2005), we used a more conservative approach by baseline correcting each epoch from -2500 to -700 ms relative to the button press in order to avoid possible contamination due to motor-related artefacts.

Statistical analysis

For K complexity, wPLI and wSMI analyses of EEG and LFPs data, repeated-measures ANOVA between conditions (endogenous, exogenous), window (before change, after change) and percept (one stream,

two streams) were performed using Bonferroni corrections for *post hoc* comparisons, and Bayes Factors of the null and alternative hypothesis were reported (Masson, 2011; Jarosz and Wiley, 2014). Statistical analyses were performed using Statistical Product and Service Solutions (SPSS, version 20.0, IBM) and open-source statistical software JASP (JASP Team (2017), version 0.8.1.1).

RESULTS

Twenty-nine healthy participants and one patient implanted with intracranial electrodes listened to a repeating pattern of three tones followed by a temporal gap. This flow of sounds is experienced either as a one-stream percept (perceptual integration) or as a two-streams percept (perceptual differentiation) (Figure 1, upper panel). Perception tends to alternate between these alternatives every few seconds (Pressnitzer and Hupé, 2006). Participants were asked to press a button as they perceived that the one-stream percept had fully changed into the two-streams percept, and a second button when perceiving the two-streams percept had fully changed into the one-stream percept (Figure 1, middle panel). As an experimental control task, we used a condition where the stimuli were physically manipulated (varying the length of the silence between tones) in order to generate two externally-driven alternating percepts (exogenous condition). Participants had to perform the same task as in endogenous condition. This control allowed us to establish the extent to which neural activity in the endogenous condition was specific to internally driven perceptual switches. It also allowed us to measure typical reaction times to percept changes with known onset times (in the control task), in order to determine suitable time windows for analysis. Furthermore, the exogenous condition allowed us to control for top-down attention in the absence of bistability by creating externally driven switches between percepts as oppose to the internally driven ones (induced endogenously).

We first investigated the dynamics of neural information integration in the gamma range (NII_γ). We compared activity during a 500-ms window before a perceptual change with activity after the change (see Materials and Methods). This approach contrasts with many previous studies of auditory bistability (Gutschalk et al., 2005; Hill et al., 2012; Szalardy et al., 2013), where the analysis windows are time-locked to the stimulus, and allowed us to concentrate in both the stable and transition periods of bistable experience. Response-locked analyses focused on how *ongoing* neural activity relates to perception. A repeated-measures ANOVA (RANOVA) revealed a significant triple interaction between condition (endogenous, exogenous), window (before change, after change), and direction (one- to two-streams, two- to one-stream) for NII_γ ($F_{1,28}$ = 5.73, P = 0.024, Cohen's d = 0.90, Bayes factor (Bf) in favour of the alternative = 2.73). Bonferroni's *post hoc* test revealed higher NII_γ in the

one-stream compared to the two-streams percept in the before-change (BC) window ($F_{1,28}$ = 7.92, P = 0.009, Cohen's d = 1.06, Bf in favour of the alternative = 6.42) (Figure 2a,c). Interestingly, ~1 s later in the after change (AC) window, NII_{γ} again showed higher values for the one-stream than the two-streams percept ($F_{1,28}$ = 5.51, P = 0.026, Cohen's d = 0.87, Bf in favour of the alternative = 2.49) (Figure 2a,c). These findings suggest that the phenomenologically integrated percept consistently involved a higher level of gamma neurophysiological integration than the phenomenologically differentiated one.

Interestingly, while NII_{γ} discriminated between conscious percepts during the endogenous condition (Figure 2a), it did not do so in the exogenous condition (BC: $F_{1,28}$ = 0.34, P = 0.561; AC: $F_{1,28}$ = 0.90, P = 0.349, Bf in favour of the null = 3.26) (Figure 2b), suggesting that frontoparietal NII_{γ} may be specifically indexing endogenously generated percepts. Furthermore, no differences were observed in the mean level of NII_{γ} between endogenous and exogenous conditions ($F_{1,28}$ = 1.39, P = 0.248, Bf in favour of the null = 2.12) or between windows ($F_{1,28}$ = 0.11, P = 0.918, Bf in favour of the null = 3.59), indicating that the overall amount of information sharing within the frontoparietal network was similar across conditions. This index of information integration was hence sensitive to endogenously driven perceptual changes and may specifically underlie the formation of conscious auditory percepts.

In order to establish the specific role of frontoparietal areas, we computed inter-hemispheric NII_{γ} between temporal electrodes. We found no reliable triple interaction in temporotemporal NII_{γ} ($F_{1,28}$ = 1.51, P = 0.228, Bf in favour of the null = 2.02) (Figure 2d,e), implying relatively specific involvement of frontoparietal networks in the emergence of endogenous auditory percepts. Finally and In addition to NII_{γ}, we investigated whether neural information integration in the alpha band (NII_{α}) dissociates between auditory percepts, as alpha activity has been previously related to perceptual bistability (Flevaris et al., 2013; Handel and Jensen, 2014). However, the ability of frontoparietal NII to track and distinguish between different endogenous percepts seems to be specifically related to the gamma range since no differences were found between percepts in frontoparietal NII_{α} ($F_{1,28}$ = 1.01, P = 0.321, Bf in favour of the null = 2.48) (Figure 2f).

We next investigated the dynamics of neural information differentiation (NID) within frontal and parietal electrodes during bistable perception (Figure 3). The RANOVA revealed a significant triple interaction between condition (endogenous, exogenous), window (before change, after change), and direction (one- to two-streams, two- to one-stream) for NID ($F_{1,28}$ = 7.05, P = 0.013, Cohen's d = 1.00, Bf in favour of the alternative = 4.57). Bonferroni's *post hoc* test revealed higher NID in the two- compared to the one-stream percept in the BC window ($F_{1,28}$ = 7.49, P = 0.011, Cohen's d = 1.03, Bf in favour of the alternative = 5.41) (Figure 3a) and a similar pattern in the AC window, showing higher

values for two streams than for one stream ($F_{1,28}$ = 6.64, P = 0.016, Bf in favour of the alternative = 3.88, Cohen's d = 0.97) (Figure 3a). These results show that the differentiated percept exhibits higher neurophysiological differentiation than the integrated one.

As was the case for NII_{γ}, information differentiation did not depend on percept in the –control- exogenous condition (B.C: $F_{1,28}$ = 0.84, P = 0.366, Bf in favour of the null = 2.66; A.C: $F_{1,28}$ = 1.94, P = 0.174, Bf in favour of the null = 1.68) (Figure 3b). Furthermore, no differences were observed in the mean level of NID between endogenous and exogenous conditions ($F_{1,28}$ = 1.39, P = 0.248, Bf in favour of the null = 2.12) or between windows ($F_{1,28}$ = 0.15, P = 0.228, Bf in favour of the null = 3.53), indicating that the overall information differentiation within the frontoparietal network was similar across conditions. Finally, no condition x window x direction interaction was observed for NID between temporal electrodes (right and left hemispheres) ($F_{1,28}$ = 3.59, P = 0.069; Bf in favour of the null = 0.86) (Figure 3c,d). In agreement with the NII results, this index of information complexity dissociated endogenous percepts. However, NID showed the opposite pattern compared to NII in terms of the direction of the effects between one and two streams, suggesting that NID is capturing a different but complementary aspect of neural information dynamics associated with conscious percepts.

In order to validate these findings in a similar manner as elsewhere (Canales-Johnson et al., 2015), we repeated the experiment in a patient implanted with intracranial electrodes for epilepsy surgery. We benefited from the high spatial resolution of intracranial recordings, allowing us to directly test the hypothesis that it is information-sharing specifically between frontal and parietal areas that differentiates between the two auditory percepts. We computed NII_{γ} on direct cortical recordings (local field potentials; LFP) between the superior parietal lobe (SPL) and middle frontal gyrus (MFG) (Table 1) obtained from the intracranial patient performing the same task as above (Figure 4a-c). As in the healthy participants, the RANOVA showed a triple interaction between (endogenous, exogenous), window (before change, after change), and direction (one- to two-streams, two- to one-stream) for NII_{γ} ($F_{1,56}$ = 36.02, P < 0.001, Cohen's d = 1.73, Bf in favour of the alternative > 100). Simple effects within the BC window showed higher NII_{γ} for the one- compared to the two-streams percept in the endogenous ($F_{1,56}$ = 18.96, P < 0.001, Cohen's d = 1.24, Bf in favour of the alternative > 100) (Figure 4b) but not the exogenous condition ($F_{1,56}$ = 0.84, P = 0.362, Bf supporting the null = 3.43) (Figure 4c). In the case of the AC window, the one-stream percept again showed higher NII_{γ} than the two-streams percept in the endogenous ($F_{1,56}$ = 6.20, P = 0.016, Bf supporting the alternative = 3.10) (Cohen's d = 0.70, Figure 4b) but not in the exogenous condition ($F_{1,56}$ = 0.33, P = 0.857, Bf in favour of the null = 4.31) (Figure 4c). Furthermore, no differences were found between these percepts in the same LFP recordings within the alpha band (NII_{α}) ($F_{1,56}$ = 0.58, P = 0.569, Bf in favour of the null = 3.84) (Figure 4f,g).

Next, we investigated NID dynamics on LFP signals in the intracranial patient within SPL and MFG (Figure 4d,e). Again, RANOVA showed a triple interaction between (endogenous, exogenous), window (before change, after change), and direction (one- to two-streams, two- to one-stream) ($F_{1,56}$ = 8.32, P = 0.008, Cohen's d = 1.13, Bf in favour of the alternative = 7.67). In agreement with the scalp EEG results, simple effects analysis within the BC window showed higher NID for the phenomenologically differentiated percept compared to the phenomenologically integrated percept in the endogenous ($F_{1,56}$ = 19.08, P < 0.001, Cohen's d = 1.71, Bf in favour of the alternative > 100) (Figure 4d) but not in the exogenous condition ($F_{1,56}$ = 2.10, P = 0.159, Bf in favour of the null = 1.97) (Figure 4e). In the case of the AC window, the two-streams percept again showed higher NID than the one-stream percept in the endogenous ($F_{1,56}$ = 10.57, P = 0.003, Cohen's d = 1.27, Bf in favour of the alternative = 20.15) (Figure 4d) but not in the control (exogenous) condition ($F_{1,56}$ = 0.49, P = 0.488, Bf in favour of the null = 4.02) (Figure 7e). These findings demonstrate strong convergent evidence between scalp EEG and direct cortical recordings, further supporting the hypothesis that phenomenology goes along with neurophysiology of conscious percepts, specifically indexed by the frontoparietal ongoing activity.

Finally, we evaluated the theoretical prediction that information dynamics but not oscillatory dynamics of brain activity underpins the emergence of conscious percepts (Koch et al., 2016). Thus, we investigated whether neural oscillatory integration (NOI) of ongoing activity might also capture the dynamics of auditory bistability. Specifically, we investigated whether frontoparietal gamma phase synchronization (Weighted Phase-Lag Index ($wPLI_\gamma$)) could differentiate between endogenous percepts. Unlike for NII_γ, RANOVA revealed no triple interaction between condition (endogenous, exogenous), window (before change, after change), and direction (one- to two-streams, two- to one-stream) for NOI_γ ($F_{(1,28)}$ = 0.12, P = 0.726, Bf in favour of the null = 3.58) (Figure 5a,b). However, a weak interaction between condition (endogenous, exogenous) and window (before change, after change) was found ($F_{(1,28)}$ = 4.22, P = 0.049, Cohen's d = 0.77, Bf in favour of the alternative = 1.50) (Figure 5c,d). Bonferroni's *post hoc* test showed that NOI_γ significantly decreased in the AC window compared to the BC window in the endogenous ($F_{(1,28)}$ = 6.51, P = 0.016, Cohen's d = 0.93, Bf in favour of the alternative = 3.73) (Fig 5c) but probably not in the exogenous condition ($F_{(1,28)}$ = 1.47, P = 0.236, Bf in favour of the null = 2.04) (Figure 5d). Furthermore, the same null result for NOI_γ between directions was observed in the intracranial patient (RANOVA (condition x window x direction): $F_{(1,56)}$ = 0.12; P = 0.726, Bf in favour of the null = 4.73) (Fig 5e,f). As with the scalp EEG, the intracranial patient showed an interaction between condition and window ($F_{(1,56)}$ = 13.51, P = 0.001, Cohen's d = 0.99, Bf in favour of the alternative = 68.09) in NOI_γ, showing a decrease in phase synchrony in the AC window compared to the BC window only in the endogenous condition (Bonferroni's *post hoc* test in endogenous condition: $F_{(1,56)}$ = 12.90, P = 0.001, Cohen's d = 0.96, Bf in favour of the alternative = 53.48; and

exogenous condition: $F_{(1,56)} = 2.16$, $P = 0.147$, Bf in favour of the null = 1.92) (Fig 5g,h) between SPL and MFG electrodes. These findings suggest that oscillatory integration does not index the identity of auditory percepts but may relate to percept stability: phase synchrony maxima occur in the BC window (before the end of a stable percept) and phase synchrony minima in the AC window (just at the onset of percept stability).

DISCUSSION

Here we demonstrate that frontoparietal information dynamics dissociates alternative conscious percepts during internally but not externally driven percepts. By studying the neural dynamics (EEG and direct cortical recordings) of theoretically-motivated information metrics, we show that empirically tractable measures of neural information integration and neural information differentiation map auditory percepts experienced either as perceptually integrated (one-stream) or differentiated (two-streams), respectively. Furthermore, phase synchronization of oscillatory gamma activity in the frontoparietal network does not differentiate between auditory percepts, nor does the information between temporal networks.

Neural correlates of consciousness and the instantiation of meaningful signatures of information integration and differentiation.

Our results expand the understanding of the neural correlates of consciousness (NCC) (Koch et al., 2016) in several manners. First, our experimental findings directly support information-based theories of consciousness (Dehaene and Changeux, 2011; Dehaene et al., 2014; Tononi et al., 2016); in their current instantiation, the Integrated Information Theory (IIT) (Tononi et al., 2016) and the Global Neuronal Workspace Theory (GNWT) (Dehaene and Changeux, 2011) of consciousness both emphasize the role of information exchange in generating conscious percepts. Although both theories conceptualize information differently, their proposed empirical indices are based on the classical Shannon-entropy information framework. Using these measures of information dynamics, our results show convergent evidence supporting both GNWT and IIT predictions by demonstrating a role of neural information in the emergence of contents of consciousness. However, the interpretation of these results in light of the IIT and GNWT is somewhat different.

Our results suggest a differential role of information integration vs. information differentiation in the emergence of conscious percepts from those proposed before. According to IIT, the neural activity associated with conscious percepts should reflect the joint presence of neurophysiological integration and neurophysiological differentiation. Under this theoretical framework, integration is expected – in

principle – to be paralleled by differentiation of neural activity. Contrary to this prediction, our results show dissociation between neurophysiological integration and neurophysiological differentiation of frontoparietal ongoing activity. Interestingly, while the phenomenologically integrated percept (one-stream) showed a relative increase in NII and relative decrease in NID, the perceptually differentiated percept (two-streams) exhibited the opposite pattern, that is, a decrease in NII and increase in NID. Together, these dissociated patterns suggest that each measure is instead directly associated with the phenomenology of conscious percepts: whereas information integration of neural activity is capturing phenomenological integration (one-stream percept), information differentiation may be capturing phenomenological differentiation (two-streams percept).

Second, we demonstrate a potential mechanistic role of information integration and differentiation in the formation of conscious percepts. Why do these measures capture the neural dynamics of conscious percepts? Coordination in the brain has been classically studied by computing phase synchronization between neural oscillations (Uhlhaas et al., 2009; Engel et al., 2013). Synchronization is a highly-ordered form of neural coordination that primarily captures the linear (or proportional) phase relationship between signals at specific frequencies (phase-locking). Thus, a mechanism of coordination-by-synchrony captures only certain regimes of neural coordination that are periodic. However, brain dynamics exhibit both a tendency to integrate information (synchronization) and a tendency for the components to differentiate information (independent function) (Dehaene and Changeux, 2011; Tognoli and Kelso, 2014; Tononi et al., 2016). During auditory bistability, conscious percepts typically alternate continuously without becoming locked into any one percept for long periods. We propose that underlying this dynamical process are ensembles of neurons that are repeatedly assembled and disassembled, and that this non-trivial dynamic might be instantiated by a mechanism of coding-by-information that captures complex, nonlinear patterns of neural activity and not merely simple proportional associations between neural signals.

Conscious auditory percepts and ongoing neural activity.

The frontoparietal patterns of neural information are a manifestation of the interaction between the external stimulation and endogenous, ongoing brain activity, as opposed to activation purely imposed by the auditory stimuli. Thus, NII and NID patterns do not merely reflect stimulus-driven neural activity but rather the intrinsic coordination of endogenous frontoparietal neural activity. Indeed, in the endogenous condition of our study, internally generated changes in neural activity were associated with changes in conscious percepts in the complete absence of any change in the auditory stimuli. In line with our results, recent studies in the visual system have shown that long-distance integration of ongoing oscillations reflects internally coordinated activity associated with conscious perception (Hipp

et al., 2012; Engel et al., 2013; Helfrich et al., 2016). Here, by directly measuring the amount of information integration and information differentiation contained in the ongoing neural activity, we demonstrate a functional role of information dynamics in the emergence of auditory conscious percepts. Our approach provides a framework for examining whether this relationship between neural and perceptual integration and differentiation generalizes, for example to the perception of ambiguous stimuli in other sensory modalities, or across modalities.

Although the pioneering electrophysiological studies supporting the active role of ongoing activity in perception and cognition date from the 70's (Freeman, 1976, 2000), over the last decade ongoing brain activity has been mainly studied in the context of "resting state networks" (Fox and Raichle, 2007). In these recent studies, fluctuations in ongoing activity between spatially segregated networks (brain regions) are correlated when a participant is not performing an explicitly defined task. In the present study, by taking advantage of the high temporal resolution of EEG and direct cortical recordings, we show that patterns of neural information are transiently coordinated during the active discrimination of internally generated auditory percepts. Furthermore, our results also allowed us to differentiate the contribution of information in frequency-space, showing that gamma but not alpha NII differentiates auditory percepts during bistable perception.

Auditory bistable perception and frontoparietal activity.

Our results also suggest a fruitful new approach to conceptualizing and investigating bistable auditory perception. We demonstrate that the dynamics of auditory conscious percepts can be associated with long-distance coordination of neural activity. For the ABA- patterns presented here, while both one-stream and two-streams percepts depend on the integration of tones over time, the latter also requires integration across tone frequency. We argue that this additional integration may draw on, or be reflected in, an increase in information sharing in ongoing frontoparietal neural activity. Additionally, maintenance of two distinct perceptual streams of sounds was associated with more differentiated neural patterns than when a single stream was perceived. How these findings relate to previous demonstrations of greater stimulus-locked activity in auditory cortex (Gutschalk et al., 2005; Hill et al., 2011; Szalardy et al., 2013) and greater BOLD response in intraparietal sulcus (Cusack, 2005; Hill et al., 2011) for two streams is presently unclear. However, the involvement of neural circuits extending beyond sensory regions is not surprising given that attention switching (Billig and Carlyon, 2015), linguistic knowledge (Billig et al., 2013), and predictability (Winkler and Schröger, 2015) have been shown to affect auditory streaming.

These findings provide convergent evidence about the role of frontoparietal networks in the dynamics of formation and maintenance of the contents of consciousness. Research in visual bistability has

focused on characterizing content-related activity predominantly in local brain areas or networks (Sterzer et al., 2009). Of those few studies that have expanded their scope to associative cortices and wider networks, one has recently proposed mechanistic accounts on visual percepts using multivariate pattern analysis (MVPA) of fMRI data (Wang et al., 2013). The results showed differential patterns of BOLD activity in high-order frontoparietal regions between visual percepts during bistable perception. The present study complements these results by showing a role for the frontoparietal network in indexing percepts in the auditory modality. Furthermore, the temporal resolution of our EEG and LFP data enabled us to characterize the fine-grained temporal dynamics of neural information integration associated with specific auditory percepts within the frontoparietal network. These results represent convergent evidence towards a possible general mechanism of information integration underlying the emergence of the contents of consciousness under invariant stimulation.

In conclusion, we have presented experimental evidence that conscious percepts may require both information integration and differentiation of ongoing neural activity in order to emerge. We have also highlighted the stark differences between fleeting endogenous percepts, where neurophysiological integration and differentiation parallel the corresponding integrated and differentiated percepts, and those that are externally triggered, for which no differences between these measures were observed. Importantly, the conceptual mapping between phenomenology and the neurophysiology that we have highlighted here should be considered as a fruitful approach for measuring the different dimensions of phenomenology in an experimentally testable manner. In light of some of the main current theoretical framework of conscious perception -IIT and GNWT- we bring additional experimental scaffolding to further understand what we have in mind at any given time.

FIGURES

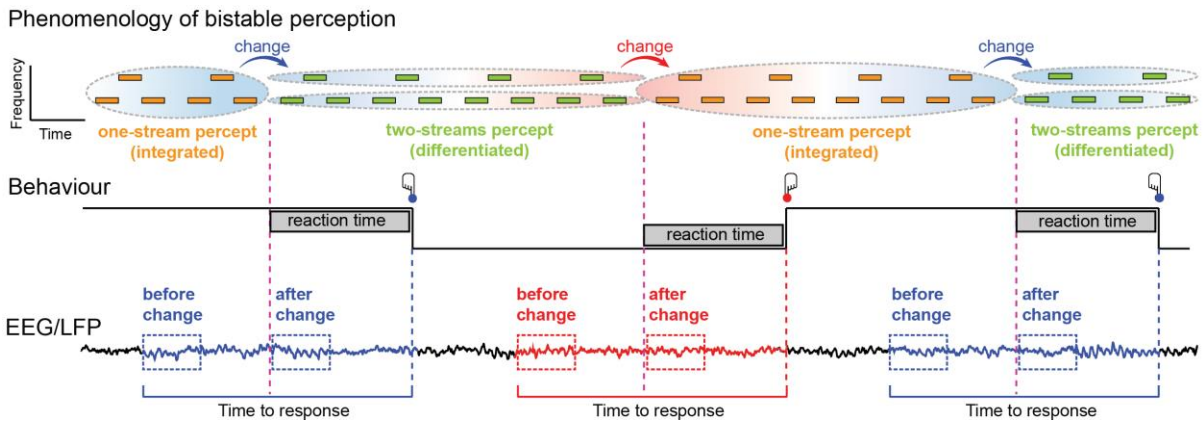

Figure 1. Experimental design and analysis of ongoing brain activity. *Top row*: Phenomenology (reported experience) during the auditory bistable illusion. Participants listened to a series of tones of two different frequencies separated by a temporal gap (see Experimental Procedures). Tones are experienced either as one stream (phenomenologically integrated percept; orange blocks surrounded by one ellipse) or as two streams (phenomenologically differentiated percept; green blocks surrounded by two ellipses). Perceptual transitions occur either in the one-stream to two-streams direction (blue arrows and blue background) or in the two-streams to one-stream direction (red arrow and red background). *Middle row*: behavioural responses during the task. Participants pressed one button when perceiving that one-stream had fully changed into two-streams percept (blue button) and another button when perceiving that two-streams had fully changed into the one-stream percept (red button). *Bottom row*: dynamical analyses and windows of interest for EEG and LFP signal analyses. Ongoing activity in during both transitions was calculated using a sliding window procedure on a fixed time window locked to the onset of the button press. Window size was calculated based on the mean reaction times (RT) in the exogenous condition (1342 ms), and the minimum duration between responses that guaranteed no overlap between RT (2500 ms) (see Materials and Methods).

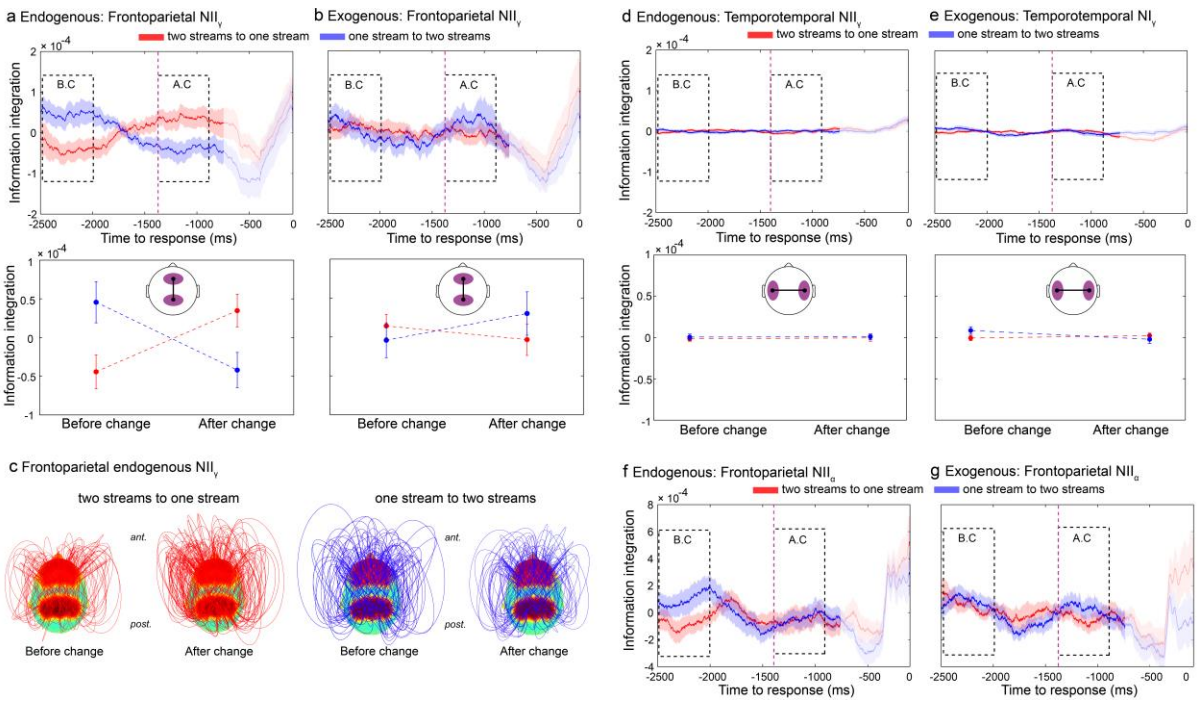

Figure 2. Frontoparietal NII dissociate alternative endogenous percepts during bistable perception. Neural dynamics of NII_γ for transitions from the two-streams to the one-stream percept (red line) and from the one-stream to the two-streams percept (blue line) for the endogenous **(a)** and exogenous (control) conditions **(b)**. Purple dashed line marks the mean reaction time (1342 ms) of the exogenous (control) condition. Auditory percepts were directly compared in two windows of interest: the before-change (BC) and the after-change (AC) windows. **(c)** Connectivity topographies for the BC and AC windows for transitions from the two-streams to the one-stream percept (left panel) and from the one-stream to the two-streams percept (right panel) averaged over participants in the endogenous condition. Red areas on the scalp indicate regions of interest (frontal and parietal electrodes, see Experimental Procedures). The height of an arc connecting two nodes indicates the strength of the NII link between them. Values are time-locked to the button press (0 ms) and baseline corrected between -2500 and -700 ms relative to button press (see Materials and Methods). Statistical analyses (bottom row) were computed on two pre-defined 500 ms windows: a BC window (-2500 to 2000 ms) and an AC window (-1342 ms to -842 ms). The onset of both windows was defined based on a control (exogenous) condition in which the stimuli physically change to generate two different percepts (see Experimental Procedures). Shaded bars (top row) and error bars (middle row) represent s.e.m. **(d,e)** Temporotemporal NII in the endogenous and exogenous conditions. **(f,g)** Frontoparietal NII in the alpha band (NII_α) during endogenous **(f)** and exogenous **(g)** conditions.

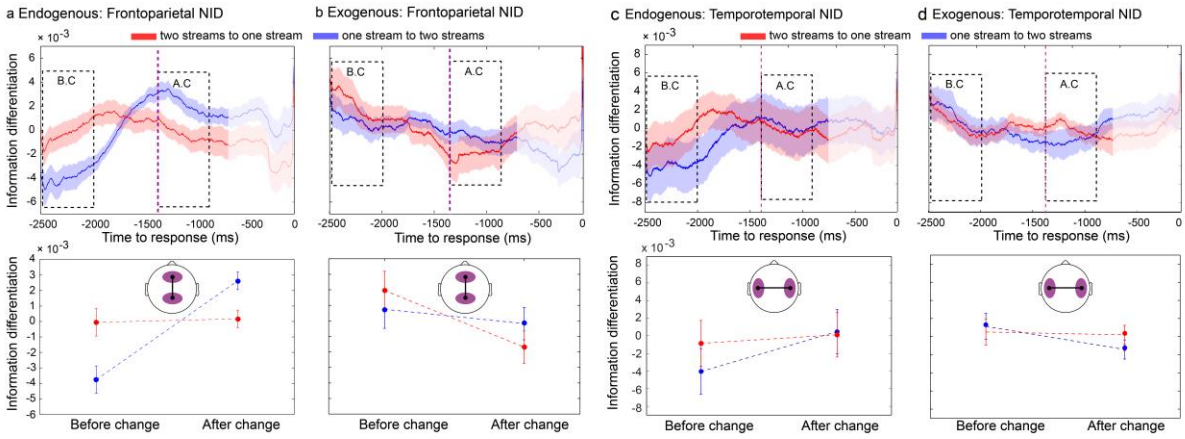

Figure 3. Frontoparietal NID dissociates alternative endogenous percepts during bistable perception. Neural dynamics of NID from the two-streams to the one-stream percept (red line) and from the one-stream to the two-streams percept (blue line) for the endogenous **(a)** and exogenous (control) conditions **(b)**. **(c,d)** Temporotemporal NID dynamics for the endogenous **(c)** and exogenous (control) conditions **(d)**. Purple dashed line marks the mean reaction time (1342 ms) of the exogenous (control) condition. Statistical analysis was performed as described in Figure 2. Shaded bars (top row) and error bars (bottom row) represent s.e.m.

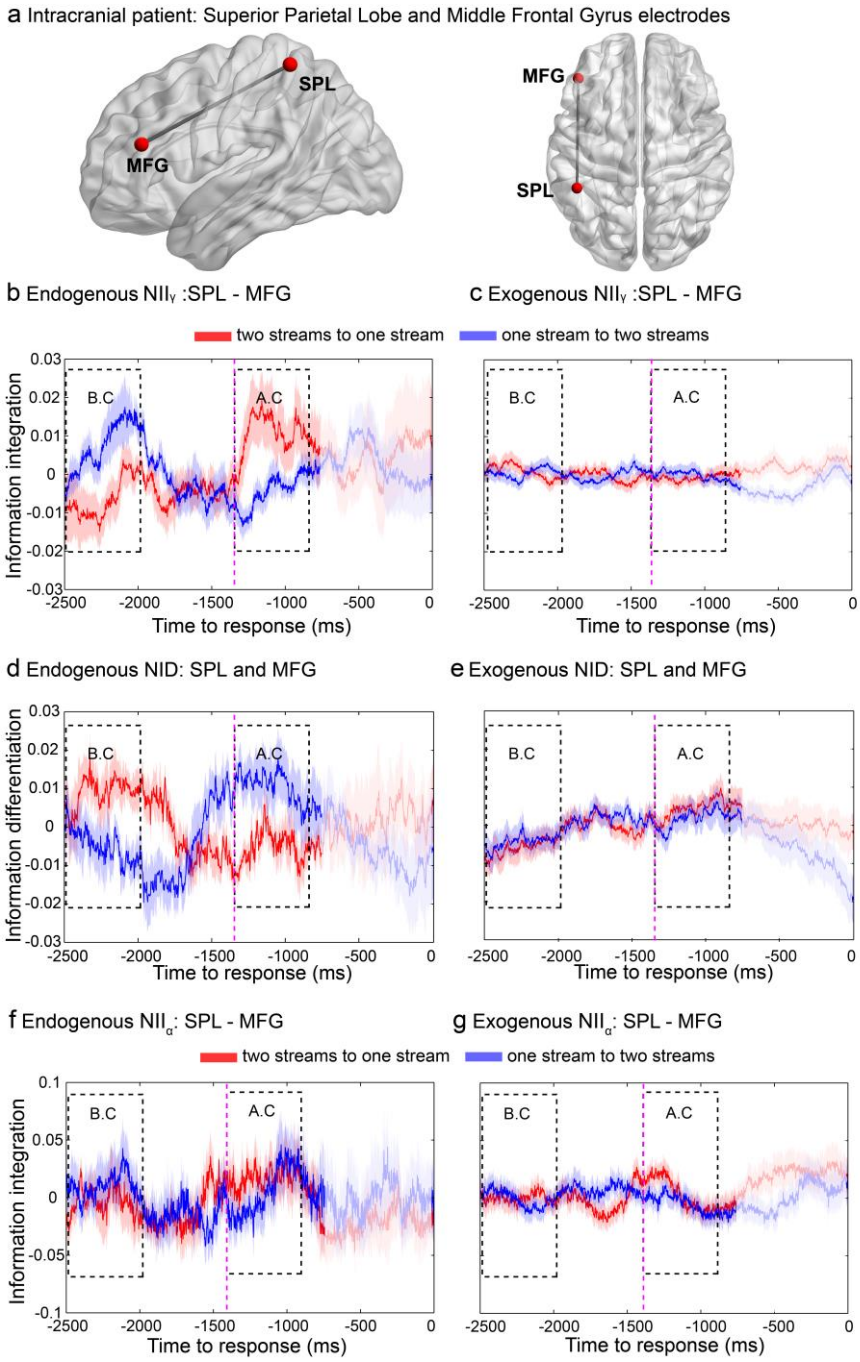

Figure 4. Frontoparietal NII and NID in local field potentials. (a) Electrodes were implanted in the left parietal lobe and left middle frontal gyrus (Table 1). Dynamics of ongoing NII_{γ} and NID of transitions from the two-streams to the one-stream percept (red line) and from the one-stream to the two-streams percept (blue line) in the endogenous **(b,d)** and exogenous **(c,e)** conditions, respectively. **(f,g)** Frontoparietal NII in the alpha band (NII_{α}) in local field potentials for the endogenous **(f)** and exogenous condition **(g)**. Purple dashed line marks the mean reaction time (1380 ms) of the exogenous (control) condition of the intracranial data. Statistical analyses were performed as explained in Figure 2. Shaded bars represent s.e.m.

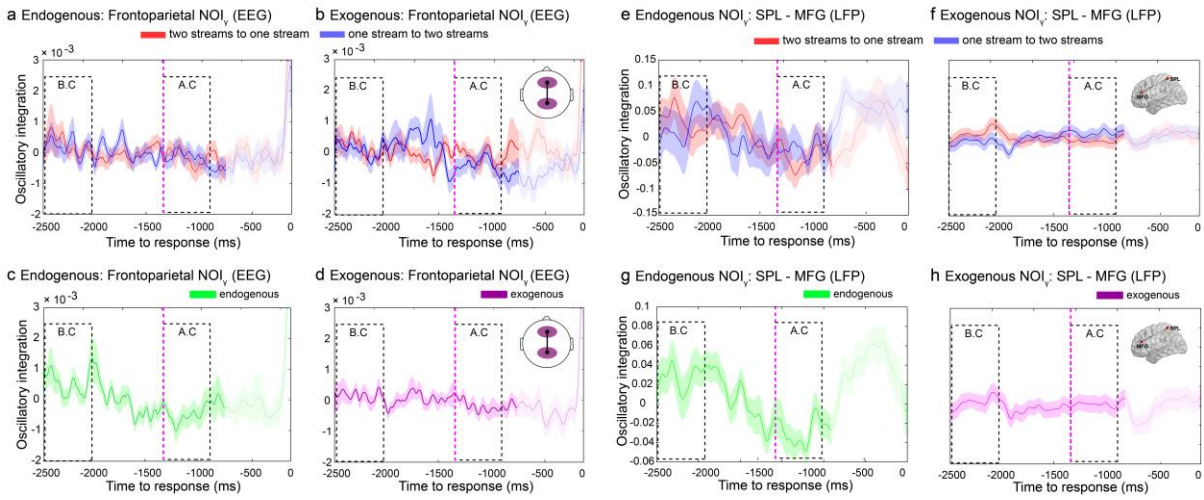

Figure 5. Frontoparietal NOI in the endogenous and exogenous conditions. Dynamics of ongoing NOI_γ from the two-streams to the one-stream percept (red line) and from the one-stream to the two-streams percept (blue line) for the endogenous **(a)** and exogenous **(b)** conditions. Ongoing NOI_γ during transitions in both directions in the endogenous **(c)** and exogenous **(d)**. Statistical analyses were performed as described in Figure 2. Shaded bars represent s.e.m. **(e-h)** Frontoparietal NOI in the alpha band (NOI_γ) in local field potentials. Ongoing NOI_γ during transitions in both directions **(e,f)** in the endogenous **(c)** and exogenous **(d)**. Statistical analyses were performed as described in Figure 2. Error bars represent s.e.m.

Table 1. Coordinates and anatomical loci of intracranial electrodes analysed

Electrode	MNI Coordinates	Cortical region (gyrus)
1	-46; 36; 20	Left Middle Frontal Gyrus
2	-46; 44; 63	Left Superior Parietal Lobe

Note: Electrodes 1 and 2 are depicted in Figure 4 and 5. SPL = Superior Parietal Lobe. MFG = Middle Frontal Gyrus.

REFERENCES

Basirat A, Sato M, Schwartz JL, Kahane P, Lachaux JP (2008) Parieto-frontal gamma band activity during the perceptual emergence of speech forms. Neuroimage 42:404–413.

Billig AJ, Carlyon RP (2015) Automaticity and Primacy of Auditory Streaming: Concurrent Subjective and Objective Measures. J Exp Psychol Hum Percept Perform

Billig AJ, Davis MH, Deeks JM, Monstrey J, Carlyon RP (2013) Lexical influences on auditory streaming. Curr Biol 23:1585–1589.

Boly M, Sasai S, Gosseries O, Oizumi M, Casali A, Massimini M, Tononi G (2015) Stimulus set meaningfulness and neurophysiological differentiation: A functional magnetic resonance imaging study. PLoS One 10.

Canales-Johnson A, Silva C, Huepe D, Rivera-Rei ??lvaro, Noreika V, Del Carmen Garcia M, Silva W, Ciraolo C, Vaucheret E, Sede??o L, Couto B, Kargieman L, Baglivo F, Sigman M, Chennu S, Ibanez A, Rodriguez E, Bekinschtein TA (2015) Auditory feedback differentially modulates behavioral and neural markers of objective and subjective performance when tapping to your heartbeat. Cereb Cortex 25:4490–4503.

Carlyon RP, Cusack R, Foxton JM, Robertson IH (2001) Effects of attention and unilateral neglect on auditory stream segregation. J Exp Psychol Hum Percept Perform 27:115–127.

Casali AG, Gosseries O, Rosanova M, Boly M, Sarasso S, Casali KR, Casarotto S, Bruno M-A, Laureys S, Tononi G, Massimini M (2013) A Theoretically Based Index of Consciousness Independent of Sensory Processing and Behavior. Sci Transl Med 5:198ra105-198ra105

Chaitin GJ (1974) Information-theoretic computation complexity. IEEE Trans Inf Theory 20:10–15

Chaitin GJ (1995) The berry paradox. No TitleComplex Syst Bin Networks 461:23–31.

Chennu S, Finoia P, Kamau E, Allanson J, Williams GB, Monti MM, Noreika V, Arnatkeviciute A, Canales-Johnson A, Olivares F, Cabezas-Soto D, Menon DK, Pickard JD, Owen AM, Bekinschtein TA (2014) Spectral Signatures of Reorganised Brain Networks in Disorders of Consciousness. PLoS Comput Biol 10.

Cusack R (2005) The intraparietal sulcus and perceptual organization. J Cogn Neurosci 17:641–651.

Dehaene S, Changeux JP (2011) Experimental and Theoretical Approaches to Conscious Processing. Neuron 70:200–227.

Dehaene S, Charles L, King JR, Marti S (2014) Toward a computational theory of conscious processing. Curr Opin Neurobiol 25:76–84.

Delorme A, Makeig S (2004) EEGLAB: an open source toolbox for analysis of single-trial EEG dynamics including independent component analysis. J Neurosci Methods 134:9–21

Doesburg SM, Kitajo K, Ward LM (2005) Increased gamma-band synchrony precedes switching of conscious perceptual objects in binocular rivalry. Neuroreport 16:1139–1142.

Engel a K, Fries P, Singer W (2001) Dynamic predictions: oscillations and synchrony in top-down processing. Nat Rev Neurosci 2:704–716

Engel AK, Gerloff C, Hilgetag CC, Nolte G (2013) Intrinsic Coupling Modes: Multiscale Interactions in Ongoing Brain Activity. Neuron 80:867–886.

Flevaris A V, Martínez A, Hillyard S a (2013) Neural substrates of perceptual integration during bistable object perception. J Vis 13:17

Foster BL, He BJ, Honey CJ, Jerbi K, Maier A, Saalmann YB (2016) Spontaneous Neural Dynamics and Multi-scale Network Organization. Front Syst Neurosci 10:7

Fox MD, Raichle ME (2007) Spontaneous fluctuations in brain activity observed with functional magnetic resonance imaging. Nat Rev Neurosci 8:700–711

Frässle S, Sommer J, Jansen A, Naber M, Einhäuser W (2014) Binocular rivalry: frontal activity relates to introspection and action but not to perception. J Neurosci 34:1738–1747

Freeman W (2000) Neurodynamics: An Exploration in Mesoscopic Brain Dynamics. Springer London.

Freeman WJ (1976) Mass action in the nervous system. Neuroscience 1:423.

Freeman WJ (2015) Mechanism and significance of global coherence in scalp EEG. Curr Opin Neurobiol 31:199–205.

Friston KJ (2006) Statistical Parametric Mapping: The Analysis of Functional Brain Images.

Gaillard R, Dehaene S, Adam C, Clémenceau S, Hasboun D, Baulac M, Cohen L, Naccache L (2009) Converging intracranial markers of conscious access. PLoS Biol 7:0472–0492.

Gutschalk A, Micheyl C, Melcher JR, Rupp A, Scherg M, Oxenham AJ (2005) Neuromagnetic correlates of streaming in human auditory cortex. J Neurosci 25:5382–5388.

Handel BF, Jensen O (2014) Spontaneous local alpha oscillations predict motion-induced blindness. Eur J Neurosci.

Helfrich RF, Knepper H, Nolte G, Sengelmann M, König P, Schneider TR, Engel AK (2016) Spectral fingerprints of large-scale cortical dynamics during ambiguous motion perception. Hum Brain Mapp.

Hill KT, Bishop CW, Yadav D, Miller LM (2011) Pattern of BOLD signal in auditory cortex relates acoustic response to perceptual streaming. BMC Neurosci 12:85

Hipp JF, Hawellek DJ, Corbetta M, Siegel M, Engel AK (2012) Large-scale cortical correlation structure of spontaneous oscillatory activity. Nat Neurosci 15:884–890.

Jarosz AF, Wiley J (2014) What are the odds? A practical guide to computing and reporting Bayes factors. J Probl Solving 7:2.

King JR, Sitt JD, Faugeras F, Rohaut B, El Karoui I, Cohen L, Naccache L, Dehaene S (2013) Information sharing in the brain indexes consciousness in noncommunicative patients. Curr Biol 23:1914–1919.

Koch C, Massimini M, Boly M, Tononi G (2016) Neural correlates of consciousness: progress and problems. Nat Rev Neurosci 17:307–321

Kolmogorov AN (1965) Three approaches to the definition of the concept of quantity of information. IEEE Trans Inf Theory 14:662–669.

Lachaux JP, Rodriguez E, Martinerie J, Varela FJ (1999) Measuring phase synchrony in brain signals. Hum Brain Mapp 8:194–208.

Le Van Quyen M, Foucher J, Lachaux J, Rodriguez E, Lutz a, Martinerie J, Varela FJ (2001) Comparison of Hilbert transform and wavelet methods for the analysis of neuronal synchrony. J Neurosci Methods 111:83–98

Lempel A, Ziev J (1976) On the Complexity of Finite Sequences. IEEE Trans Inf Theory 22:75–82.

Levy J, Vidal JR, Fries P, Démonet J-F, Goldstein A, Demonet J-F, Goldstein A (2015) Selective Neural Synchrony Suppression as a Forward Gatekeeper to Piecemeal Conscious Perception. Cereb Cortex:1–13

Masson MEJ (2011) A tutorial on a practical Bayesian alternative to null-hypothesis significance testing. Behav Res Methods 43:679–690.

Melloni L, Molina C, Pena M, Torres D, Singer W, Rodriguez E (2007) Synchronization of neural activity across cortical areas correlates with conscious perception. J Neurosci 27:2858–2865

Mill RW, Bohm TM, Bendixen A, Winkler I, Denham SL (2013) Modelling the Emergence and Dynamics of Perceptual Organisation in Auditory Streaming. PLoS Comput Biol 9.

Noreika V, Canales-Johnson A, Koh J, Taylor M, Massey I, Bekinschtein TA (2015) Intrusions of a drowsy mind: Neural markers of phenomenological unpredictability. Front Psychol 6.

Oizumi M, Albantakis L, Tononi G (2014) From the Phenomenology to the Mechanisms of Consciousness: Integrated Information Theory 3.0. PLoS Comput Biol 10.

Oostenveld R, Fries P, Maris E, Schoffelen JM (2011) FieldTrip: Open source software for advanced analysis of MEG, EEG, and invasive electrophysiological data. Comput Intell Neurosci 2011.

Parkkonen L, Andersson J, Hämäläinen M, Hari R (2008) Early visual brain areas reflect the percept of an ambiguous scene. Proc Natl Acad Sci U S A 105:20500–20504.

Pressnitzer D, Hupé JM (2006) Temporal Dynamics of Auditory and Visual Bistability Reveal Common Principles of Perceptual Organization. Curr Biol 16:1351–1357.

Rorden C, Brett M (2000) Stereotaxic Display of Brain Lesions. Behav Neurol 12:191–200

Salomon D (2004) Data compression: the complete reference. Springer Science & Business Media.

Sarasso S, Boly M, Napolitani M, Gosseries O, Charland-Verville V, Casarotto S, Rosanova M, Casali AG, Brichant JF, Boveroux P, Rex S, Tononi G, Laureys S, Massimini M (2015) Consciousness and complexity during unresponsiveness induced by propofol, xenon, and ketamine. Curr Biol 25:3099–3105.

Schartner M, Seth A, Noirhomme Q, Boly M, Bruno MA, Laureys S, Barrett A (2015) Complexity of multi-dimensional spontaneous EEG decreases during propofol induced general anaesthesia. PLoS One 10.

Schartner MM, Carhart-Harris RL, Barrett AB, Seth AK, Muthukumaraswamy SD (2017) Increased spontaneous MEG signal diversity for psychoactive doses of ketamine, LSD and psilocybin. Sci Rep 7.

Schroger E, Bendixen A, Denham SL, Mill RW, Bohm TM, Winkler I (2014) Predictive regularity representations in violation detection and auditory stream segregation: From conceptual to computational models. Brain Topogr 27:565–577.

Sitt JD, King JR, El Karoui I, Rohaut B, Faugeras F, Gramfort A, Cohen L, Sigman M, Dehaene S, Naccache L (2014) Large scale screening of neural signatures of consciousness in patients in a vegetative or minimally conscious state. Brain 137:2258–2270.

Snyder JS, Gregg MK, Weintraub DM, Alain C (2012) Attention, awareness, and the perception of auditory scenes. Atten Conscious Differ senses:95.

Stam CJ, Nolte G, Daffertshofer A (2007) Phase lag index: Assessment of functional connectivity from multi channel EEG and MEG with diminished bias from common sources. Hum Brain Mapp 28:1178–1193.

Sterzer P, Kleinschmidt A, Rees G (2009) The neural bases of multistable perception. Trends Cogn Sci 13:310–318.

Szalardy O, Bohm TM, Bendixen A, Winkler I (2013) Event-related potential correlates of sound organization: Early sensory and late cognitive effects. Biol Psychol 93:97–104.

Tognoli E, Kelso JAS (2014) The Metastable Brain. Neuron 81:35–48.

Tononi G, Boly M, Massimini M, Koch C (2016) Integrated information theory: from consciousness to its physical substrate. Nat Rev Neurosci 17:450–461

Uhlhaas PJ, Pipa G, Lima B, Melloni L, Neuenschwander S, Nikolic D, Singer W (2009) Neural synchrony in cortical networks: history, concept and current status. Front Integr Neurosci 3:17

Varela F, Lachaux JP, Rodriguez E, Martinerie J (2001) The brainweb: phase synchronization and large-scale integration. Nat Rev, Neurosci 2:229–239.

Vinck M, Oostenveld R, Van Wingerden M, Battaglia F, Pennartz CMA (2011) An improved index of phase-synchronization for electrophysiological data in the presence of volume-conduction, noise and sample-size bias. Neuroimage 55:1548–1565.

Wang M, Arteaga D, He BJ (2013) Brain mechanisms for simple perception and bistable perception. Proc Natl Acad Sci 110:E3350–E3359

Winkler I, Schröger E (2015) Auditory perceptual objects as generative models: Setting the stage for communication by sound. Brain Lang 148:1–22.

Xia M, Wang J, He Y (2013) BrainNet Viewer: A Network Visualization Tool for Human Brain Connectomics. PLoS One 8.